Coupled Systems Mechanics, *Vol. 4, No. 3(2015) 251-262*
DOI: http://dx.doi.org/10.12989/csm.2015.4.3.251

Dynamical behaviour of electrically actuated microcantilevers

Hamed Farokhi[1] and Mergen H. Ghayesh[*2]

[1]*Department of Mechanical Engineering, McGill University, Montreal, Quebec, Canada H3A 0C3*
[2]*School of Mechanical, Materials and Mechatronic Engineering, University of Wollongong, NSW 2522, Australia*

(Received September 6, 2014, Revised July 17, 2015, Accepted August 18, 2015)

Abstract. The current paper aims at investigating the nonlinear dynamical behaviour of an electrically actuated microcantilever. The microcantilever is excited by a combination of AC and DC voltages. The nonlinear equation of motion of the microcantilever is obtained by means of force and moment balances. A high-dimensional Galerkin scheme is then applied to reduce the equation of motion to a discrete model. A numerical technique, based on the pseudo-arclength continuation method, is used to solve the discretized model. The electrostatic deflection of the microcantilever and static pull-in instabilities, due to the DC voltage, are analyzed by plotting the so-called DC voltage-deflection curves. At the simultaneous presence of the DC and AC voltages, the nonlinear dynamical behaviour of the microcantilever is analyzed by plotting frequency-response and force-response curves.

Keywords: microcantilevers; electrically actuated; pull-in instability; dynamical behaviour

1. Introduction

Microcantilevers are present in a wide spectrum of applications, for example, in capacitive accelerometers, micropumps, capacitive sensors, resonators, and microswitches (Zengerle *et al*. 1992, Saif *et al*. 1999, Bao *et al*. 2000, Ibrahimbegović and Al Mikdad 2000, Ansari *et al*. 2012, Ansari *et al*. 2013, Ibrahimbegović *et al*. 2013, Ngo *et al*. 2014). Between all forms of actuation, the electric actuation is the preferred one; it is usually comprised of DC and AC components. Under an electrostatic actuation, due to the DC voltage, the microcantilever deflects to a new non-trivial equilibrium configuration. The application of the AC voltage over the DC voltage causes the microcantilever to oscillate over the deflected configuration. When the applied potential difference exceeds a threshold, known as the pull-in voltage, the elastic restoring force can no longer withstand the electric excitations and the system fails and establishes a physical contact and collapse.

The *static* deflection of microbeams, due to the DC voltage, and the corresponding pull-in have been examined by many researchers and are still of interest today. Only a few studies are reviewed here, specifically those published in recent years. For instance, the pull-in instability of electrostatically actuated beams with different boundary conditions was examined by Pamidighantam *et al.* (2002). Hu *et al*. (2010) conducted a pull-in analysis of an electrostatically

∗Corresponding author, Dr., E-mail: mergen@uow.edu.au

http://www.techno-press.org/?journal=csm&subpage=7 ISSN: 2234-2184 (Print), 2234-2192 (Online)

actuated geometrically nonlinear initially curved microbeams. Baghani (2012) contributed to the field by analyzing the size dependent response of microcantilevers actuated by a DC voltage. Wang *et al.* (2012) examined the pull-in characteristics of an electrostatically actuated microbeam.

There are few studies in the literature that considered both the DC and AC components of the electric actuation (Ghayesh *et al*. 2013). For example, Abdel-Rahman and Nayfeh (2003) examined the response of a deformable electrode of a sensor subjected to superharmonic and subharmonic electric actuations. Younis *et al*. (2003) proposed a reduced-order model to characterize the statics and dynamics of electrically actuated microbeams. Alsaleem *et al.* (2009) conducted an experimental investigation on the nonlinear resonances and dynamic pull-in instability of a resonator. Jia *et al*. (2012) contributed to the field by performing an analytical investigation on the nonlinear dynamics of electrically actuated micro-switches tuned near a resonance region. Kim *et al*. (2012) investigated the primary, subharmonic, and superharmonic resonances of a microcantilever by means of the method of multiple timescales.

Most of the studies in the literature employed assumed-mode methods to discretize the partial differential equation of motion into a set of ordinary differential equations. As reported in Ref. (Younis 2011), for an *electrostatic* analysis of a system only subject to a DC voltage, at least four modes are required. When an AC voltage is superimposed over the DC voltage, the number of modes required in the discretization increases in order to obtain converged and reliable dynamical results. Therefore, the necessity of developing a high-dimensional discretized model (Farokhi *et al*. 2013, Farokhi *et al*. 2013, Ghayesh *et al*. 2013a, Ghayesh *et al*. 2013b, Ghayesh *et al*. 2013c, Ghayesh and Amabili 2014) capable of analyzing the static and dynamic behaviour of the system accurately is seriously felt. To this end, the present paper examines the motion characteristics of an electrically actuate microcantilever using a high-dimensional discretization. The electrical field consists of a DC voltage along with a harmonic AC voltage. Employing an 8-mode Galerkin scheme, the nonlinear partial differential equation of motion is discretized and then the pseudo-arclength continuation technique is utilized to solve the discretized equations. First, the static analysis is conducted in order to obtain the deflected configuration of the microcantilever due to the DC voltage. Second, the resonant response of the microcantilever is examined under the harmonic AC actuation, around the deflected configuration, by constructing the frequency-response and force-response curves.

2. Model development

Shown in Fig. 1 is a microcantilever (deformable electrode) of length L, width b, flexural stiffness EI, axial stiffness EA, and thickness h, separated by a dielectric spacer with an initial gap d from a stationary electrode modelled as a ground plane; the dielectric constant of the gap medium is denoted by ε. The microcantilever is actuated by an electric force in the form of combined DC and AC voltages; i.e., $V_{DC}+V_{AC}\cos(\omega t)$, where V_{DC} stands for the polarization voltage or static loading, V_{AC} represents the amplitude of the AC voltage, and ω denotes the frequency of the AC voltage (i.e., the excitation frequency).

The transverse displacement of the centreline of the microcantilever is denoted by $w(x,t)$. For an Euler-Bernoulli microcantilever, the application of force and moment balances for an infinitesimal element of the microcantilever gives (Ghayesh *et al*. 2011, Ghayesh *et al*. 2012)

$$\frac{\partial}{\partial x}\left(N\frac{\partial w}{\partial x}\right)-\frac{\partial^2 M}{\partial x^2}+F=\rho A\frac{\partial^2 w}{\partial t^2} \tag{1a}$$

$$F=\frac{\varepsilon b\left[V_{DC}+V_{AC}\cos(\omega t)\right]^2}{2(d-w)^2},\quad M=EI\frac{\partial^2 w}{\partial x^2},\quad N=\frac{1}{2}EA\left(\frac{\partial w}{\partial x}\right)^2 \tag{1b}$$

with F, M, and N representing the electric load, the bending moment, and the axial force, respectively.

Substitution of Eq. 1(b) into Eq. 1(a) as well as formulating a viscous-type damping gives

$$\rho A\frac{\partial^2 w}{\partial t^2}+\mu\frac{\partial w}{\partial t}+EI\frac{\partial^4 w}{\partial x^4}=\frac{3}{2}EA\frac{\partial^2 w}{\partial x^2}\left(\frac{\partial w}{\partial x}\right)^2+\frac{\varepsilon b\left[V_{DC}+V_{AC}\cos(\omega t)\right]^2}{2(d-w)^2} \tag{2}$$

where μ is the damping coefficient.

Substitution of the following dimensionless parameters into Eq. (2)

$$x^*=\frac{x}{L},\ w^*=\frac{w}{d},\ \alpha_1=6\left(\frac{d}{h}\right)^2,\ t^*=t\sqrt{\frac{EI}{\rho AL^4}},\ \alpha_2=\frac{6\varepsilon L^4}{Eh^3d^3},\ \Omega=\omega\sqrt{\frac{\rho AL^4}{EI}},\ \mu^*=\frac{\mu L^4}{EI}\sqrt{\frac{EI}{\rho AL^4}} \tag{3}$$

and dropping the asterisk notation for the sake of brevity renders the equation of motion dimensionless as

$$\frac{\partial^2 w}{\partial t^2}+\mu\frac{\partial w}{\partial t}+\frac{\partial^4 w}{\partial x^4}-3\alpha_1\frac{\partial^2 w}{\partial x^2}\left(\frac{\partial w}{\partial x}\right)^2-\frac{\alpha_2\left[V_{DC}+V_{AC}\cos(\Omega t)\right]^2}{(1-w)^2}=0 \tag{4}$$

with the following dimensionless boundary conditions

$$w\big|_{x=0}=\frac{\partial w}{\partial x}\big|_{x=0}=0,\ \frac{\partial^2 w}{\partial x^2}\big|_{x=1}=\frac{\partial^3 w}{\partial x^3}\big|_{x=1}=0 \tag{5}$$

The denominator in Eq. (4) may be approximated by the Taylor expansion up to minimum order of twenty to avoid numerical error. However, in the current study, this term is handled as it appears; this makes the run-time significantly higher but leads to accurate and converged results.

In order to reduce the continuous system of Eq. (4) into a set of discretized equations with finite degrees of freedom, the Galerkin method is utilized. Hence, the transverse displacement is approximated through use of the following series expansion (Ghayesh 2012)

$$w(x,t)=\sum_{r=1}^{N}\phi_r(x)q_r(t) \tag{6}$$

where N is the number of degrees of freedom, $q_r(t)$ represents the rth generalized coordinate, and $\phi_r(x)$ denotes the rth mode shape satisfying the boundary conditions of Eq. (5). Inserting Eq. (6) into Eq. (4), multiplying the resultant equations by the corresponding eigenfunction and integrating over the spatial domain results in the following set of second-order nonlinear ordinary differential equations with time-dependent terms both at numerators and denominators

$$\sum_{j=1}^{N}\left(\int_0^1 \phi_i\phi_j dx\right)\ddot{q}_j + \mu\sum_{j=1}^{N}\left(\int_0^1 \phi_i\phi_j dx\right)\dot{q}_j = 3\alpha_1\sum_{j=1}^{N}\sum_{k=1}^{N}\sum_{i=1}^{N}\left[\int_0^1 \phi_i\phi_j''\phi_k'\phi_l' dx\right]q_j q_k q_l$$
$$+\alpha_2\left[V_{DC}+V_{AC}\cos(\Omega t)\right]^2\int_0^1\left[\left(1-\sum_{i=1}^{N}\phi_j q_j\right)^{-2}\phi_i\right]dx = 0, \qquad \text{with } i, j = 1, 2, ..., N \tag{7}$$

where the dot and prime notations represent the differentiations with respect to the dimensionless time and axial coordinate, respectively.

Eq. (7) consists of N second-order nonlinear ordinary differential equations. In order to solve these equations numerically, a change of variables $x_i = q_i$ is employed to convert these equations into a set of 2N first-order nonlinear ordinary differential equations (Ghayesh 2012, Ghayesh *et al*. 2012). The linear parts of these 2N equations are then solved by means of an eigenvalue analysis in order to obtain the linear natural frequencies of the microcantilever over the deflected configuration (due to the DC voltage). The pseudo-arclength continuation technique is then employed in order to obtain the static deflection due to the DC voltage as well as the dynamic oscillations due to the AC voltage.

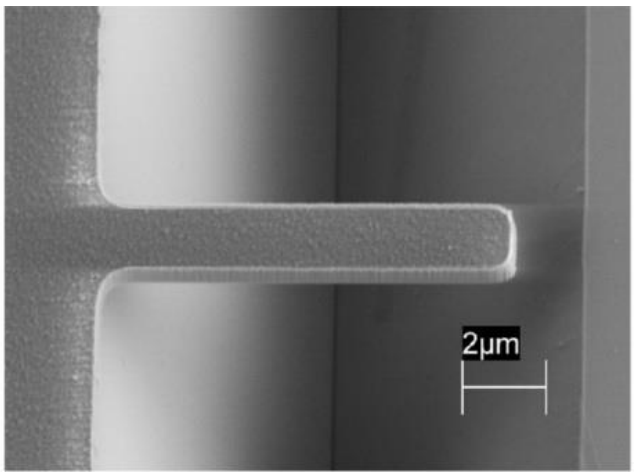

(a)

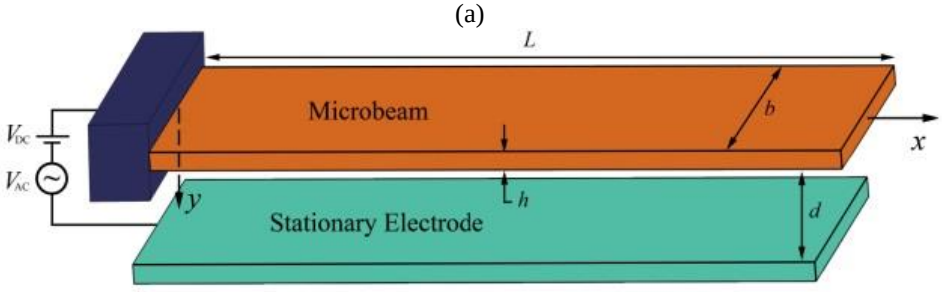

(b)

Fig. 1 (a) Electrically actuated microcantilever (Kim *et al*. 2012) and (b) schematic representation of an electrically actuated microcantilever

3. Nonlinear electrostatic deflection

The nonlinear electrostatic deflection of the microcantilever due to the DC voltage is obtained in this section; V_{AC} is set to zero. The DC voltage is increased as the bifurcation parameter and the microcantilever deflection is obtained. Fig. 2 shows the electrostatic deflection of the microcantilever through (a) the amplitude of the first generalized coordinate and (b) the deflection amplitude of the free end (tip) of the microcantilever for the following system parameters: α_1=2.8 and α_2=3.0. As seen in this figure, the tip deflection amplitude increases with V_{DC} until reaching a critical value named as pull-in voltage, where a limit point bifurcation occurs and the solution becomes unstable. It can also be seen that the unstable branch is not the symmetric counterpart of the stable solution branch, since the electrostatic pull-in occurs when the tip displacement is in the vicinity of 0.4, rather than 0.5.

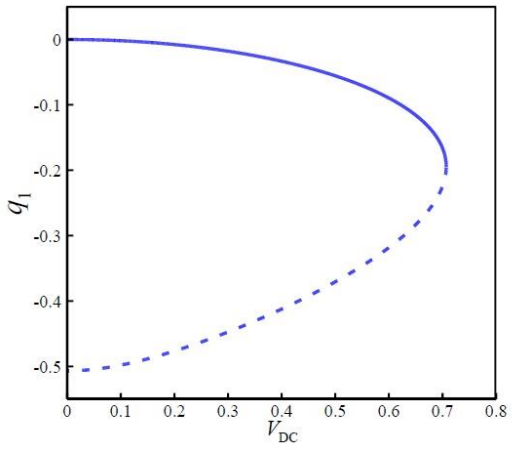

(a)

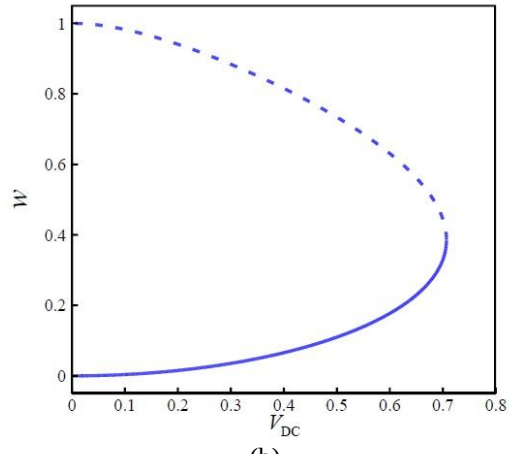

(b)

Fig. 2 Electrostatic deflection of the microcantilever actuated by an electrostatic excitation load V_{DC}: (a) the amplitude of the first generalized coordinate and (b) the amplitude of the deflection at the tip of the microcantilever

Fig. 3 illustrates the influence of α_1 on the electrostatic deflection curves of the system; the value of α_2 is set to 3.0. As seen, for larger values of α_1, the pull-in takes place at lower V_{DC}. A snap-through motion is predicated for the case with α_1 =70.

The effect of α_2 on the electrostatic deflection of the microcantilever is highlighted in Fig. 4, through (a) the deflection amplitude of the q_1 motion and (b) the deflection amplitude of the free-end (tip) of the microcantilever; the value of α_1 is set to 2.8. As seen in this figure, the larger the value of α_2 is, the smaller the pull-in voltage becomes.

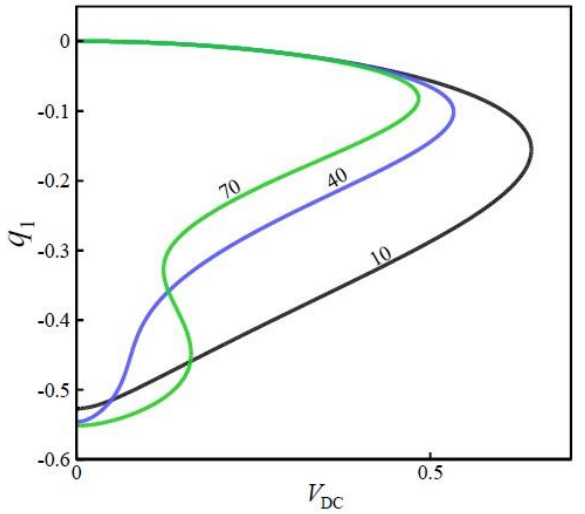

(a)

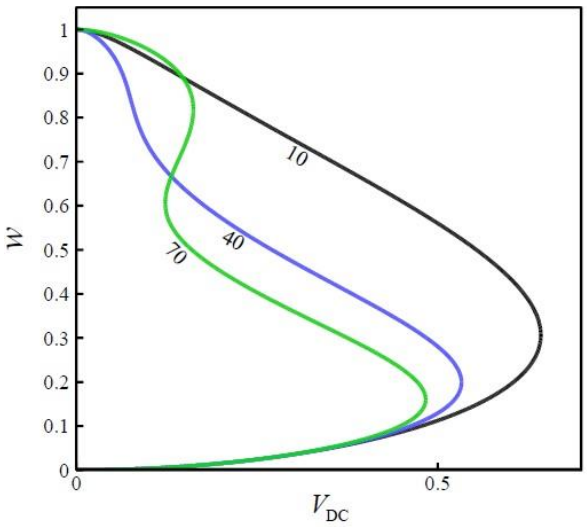

(b)

Fig. 3 Electrostatic deflection of the microcantilever for several values of α_1: (a) deflection amplitude of the q_1 motion and (b) deflection amplitude of the tip of the microcantilever. The values of α_1 are denoted on the curves

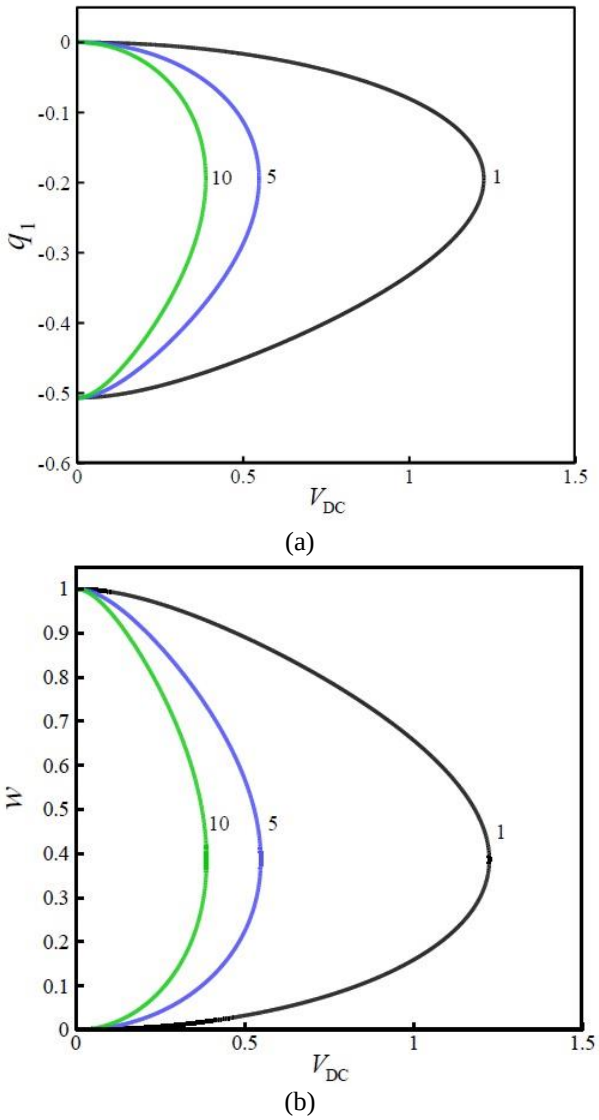

Fig. 4 Electrostatic deflection of the microcantilever for several values of α_2: (a) deflection amplitude of the q_1 motion and (b) deflection amplitude of the tip of the microcantilever. The values of α_2 are denoted on the curves

4. Nonlinear electrodynamic oscillations

This section analyzes the nonlinear electrodynamic oscillations of the microcantilever due to the AC voltage; in other words, the DC voltage is applied to the microcantilever causing it to deflect to a new configuration; the AC voltage is applied (with V_{AC} amplitude and Ω frequency) which causes it to oscillate over the deflected configuration (due to the DC voltage). The case

study in this section is for a microcantilever with α_1=3.7, α_2=3.9, and μ=0.0239.

Application of an eigenvalue analysis upon the linear terms of the deflected microcantilever (due to the DC voltage) gives ω_1=3.3926; this value is the same for all figures of this section.

Fig. 5 shows the maximum oscillation amplitude as the excitation frequency Ω (i.e., the frequency of the AC voltage) varies. For this figure, V_{DC} and V_{AC} are set to 0.3003 and 0.0040, respectively. Sub-figures (a) and (b) illustrate the maximum oscillation amplitude of the q_1 motion and the tip of the microcantilever, respectively.

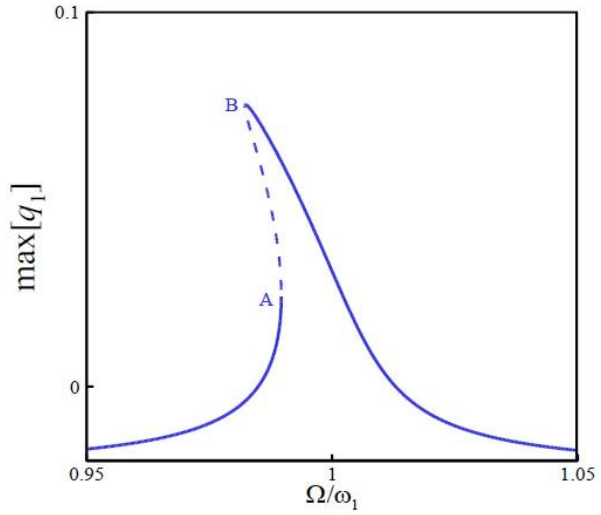

(a)

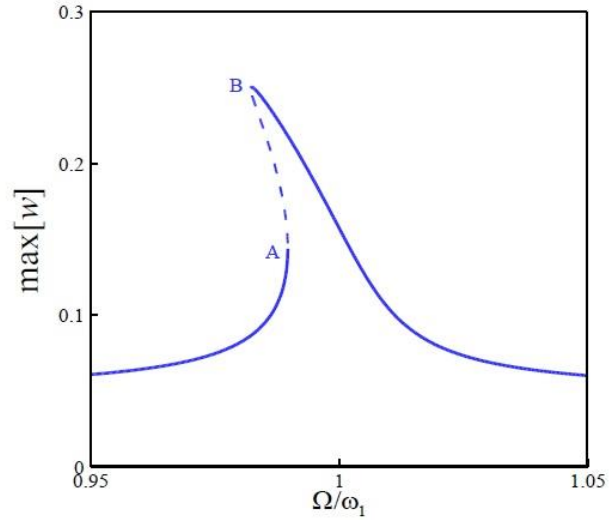

(b)

Fig. 5 Maximum oscillation amplitude versus the AC actuation frequency for fixed V_{DC} and V_{AC}: (a) for the q_1 motion and (b) for the tip of the microcantilever. Solid and dashed lines represent the stable and unstable solutions, respectively

As seen in the figure, the nonlinear behaviour of the microcantilever is a softening type with two limit point bifurcations at points A and B with Ω=0.9896ω_1 and Ω=0.9822ω_1, respectively; the solution branch between these two points is unstable. The bifurcation point A is responsible for a jump from the lower amplitude solution branch to the higher-amplitude one.

Fig. 6 shows the maximum oscillation amplitude as the AC actuation amplitude (V_{AC}) is varied; the values for V_{DC} and Ω are set to 0.3003 and 0.98ω_1, respectively. As V_{AC} is increased from zero, the oscillation amplitude increases accordingly until point A (V_{AC} =0.0097) is hit, where the first instability occurs via a limit point bifurcation; at this point, a jump occurs to the upper stable branch.

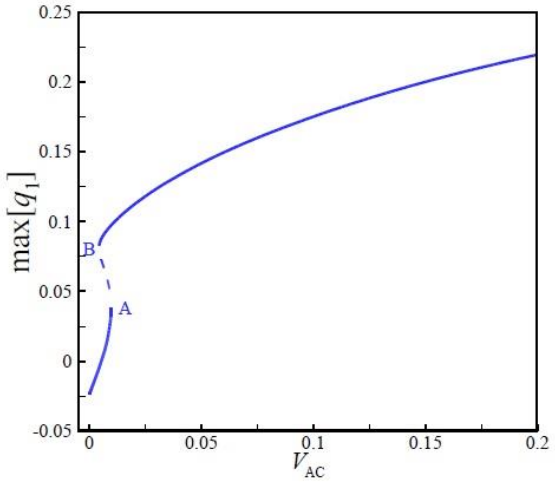

(a)

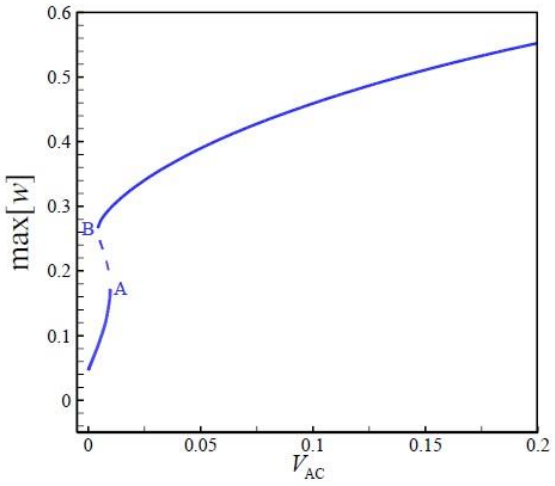

(b)

Fig. 6 Maximum oscillation amplitude versus the AC actuation amplitude for fixed V_{DC} and Ω: (a) for the q_1 motion and (b) for the tip of the microcantilever. Solid and dashed lines represent the stable and unstable solutions, respectively

Decreasing V_{AC} from 0.2, the oscillation amplitude decreases accordingly until reaching point B (V_{AC} =0.0043), where another limit point bifurcation occurs, accompanied by a jump to the lower-amplitude solution branch.

Increasing the actuation frequency Ω, to $1.02\omega_1$, from $0.9800\omega_1$ in Fig. 6, the curves of Fig. 7 is generated. It is seen that due to increased actuation frequency Ω, the unstable solution branch and bifurcation points diminish; in other words, the system displays only a stable periodic response for the ranges of V_{AC} studied here.

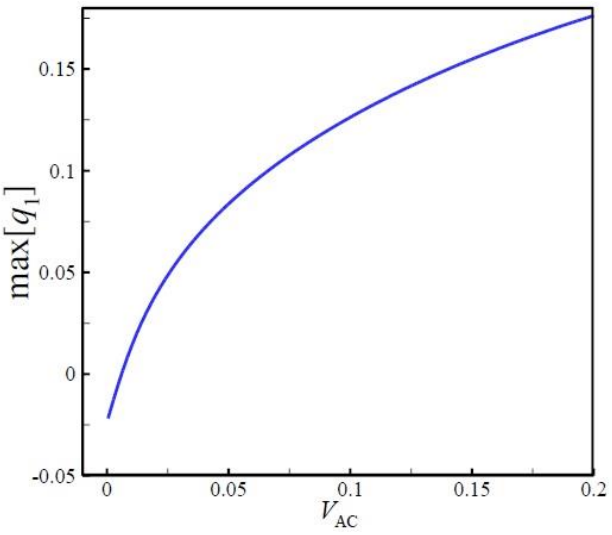

(a)

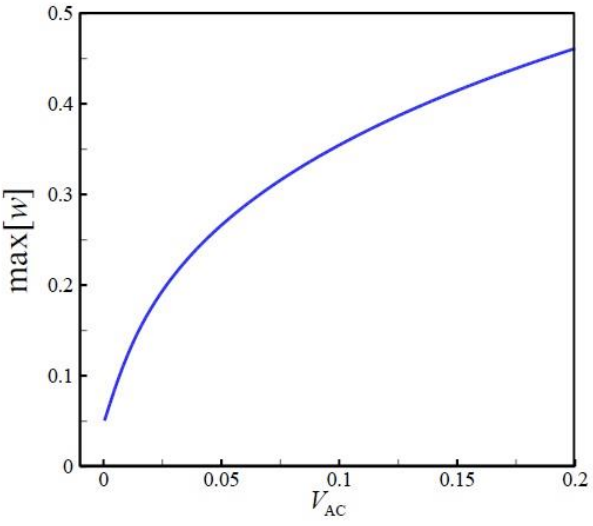

(b)

Fig. 7 Maximum oscillation amplitude versus the AC actuation amplitude for fixed V_{DC} and Ω: (a) for the q_1 motion and (b) for the tip of the microcantilever

5. Conclusions

The nonlinear dynamical behaviour of an electrically actuated microcantilever has been examined numerically in this paper. The electric actuation is comprised of AC and DC voltages. The geometrically nonlinear equation governing the transverse motion of the microcantilever was obtained by means of force and moment balances. The application of the Galerkin method on the equation of motion resulted in a high-dimensional set of ordinary differential equations which were solved using the pseudo-arclength continuation technique for both electrostatic and electrodynamic deflections of the microcantilever in order to analyze pull-in instabilities as well as nonlinear responses.

The static analysis showed that the unstable branch is not a symmetric counterpart of the stable solution branch. It was also shown that increasing either α_1 or α_2 results in a lower pull-in voltage and hence decreases the resistance of the system against the pull-in instability.

The dynamic analysis, on the other hand, revealed that the microcantilever displays a softening-type nonlinear behaviour; the frequency-response curves of the system showed that two limit point bifurcations occur by varying the actuation frequency. The force-response curves of the system revealed that for a system with actuation frequency less than ω_1, two limit point bifurcations occur as the AC voltage is varied; the force-response curve of the system with actuation frequency higher than ω_1, on the other hand, shows only stable response without any limit point bifurcations.

References

Abdel-Rahman, E.M. and Nayfeh, A.H. (2003), "Secondary resonances of electrically actuated resonant microsensors", *J. Micromech. Microeng.*, **13**(3), 491-501.

Alsaleem, F.M., Younis, M.I. and Ouakad, H.M. (2009), "On the nonlinear resonances and dynamic pull-in of electrostatically actuated resonators", *J. Micromech. Microeng.*, **19**(4), 045013.

Ansari, R., Faghih Shojaei, M., Gholami, R., Mohammadi, V. and Darabi, M. (2012), "Thermal postbuckling behavior of size-dependent functionally graded timoshenko microbeams", *Int. J. Nonlinear Mech.*, **50**, 127-135.

Ansari, R., Faghih Shojaei, M., Mohammadi, V., Gholami, R. and Darabi, M.A. (2013), "Buckling and postbuckling behavior of functionally graded Timoshenko microbeams based on the strain gradient theory", *J. Mech. Mater. Struct.*, **7**(10), 931-949.

Baghani, M. (2012), "Analytical study on size-dependent static pull-in voltage of microcantilevers using the modified couple stress theory", *Int. J. Eng. Sci.*, **54**, 99-105.

Bao, M., Yang, H., Yin, H. and Shen, S. (2000), "Effects of electrostatic forces generated by the driving signal on capacitive sensing devices", *Sensor. Actuat. - A*, **84**(3), 213-219.

Farokhi, H., Ghayesh, M. and Amabili, M. (2013), "Nonlinear resonant behavior of microbeams over the buckled state", *Appl. Phys. A*, 1-11.

Farokhi, H., Ghayesh, M.H. and Amabili, M. (2013), "Nonlinear dynamics of a geometrically imperfect microbeam based on the modified couple stress theory", *Int. J. Eng. Sci.*, **68**, 11-23.

Ghayesh, M. (2012a), "Stability and bifurcations of an axially moving beam with an intermediate spring support", *Nonlinear Dyn.*, **69**(1-2), 193-210.

Ghayesh, M. (2012b), "Subharmonic dynamics of an axially accelerating beam", *Arch. Appl. Mech.*, **82**(9), 1169-1181.

Ghayesh, M., Farokhi, H. and Amabili, M. (2013), "Coupled nonlinear size-dependent behaviour of microbeams", *Appl. Phys. A*, **112**(2), 329-338.

Ghayesh, M.H. and Amabili, M. (2014), "Coupled longitudinal-transverse behaviour of a geometrically imperfect microbeam", *Compos. Part B: Eng.*, **60**, 371-377.
Ghayesh, M.H., Amabili, M. and Farokhi, H. (2013a), "Nonlinear forced vibrations of a microbeam based on the strain gradient elasticity theory", *Int. J. Eng. Sci.*, **63**(0), 52-60.
Ghayesh, M.H., Amabili, M. and Farokhi, H. (2013b), "Three-dimensional nonlinear size-dependent behaviour of Timoshenko microbeams", *Int. J. Eng. Sci.*, **71**, 1-14.
Ghayesh, M.H., Farokhi, H. and Amabili, M. (2013c), "Nonlinear behaviour of electrically actuated MEMS resonators", *Int. J. Eng. Sci.*, **71**, 137-155.
Ghayesh, M.H., Kazemirad, S. and Amabili, M. (2012), "Coupled longitudinal-transverse dynamics of an axially moving beam with an internal resonance", *Mech. Mach. Theory*, **52**, 18-34.
Ghayesh, M.H., Kazemirad, S. and Darabi, M.A. (2011), "A general solution procedure for vibrations of systems with cubic nonlinearities and nonlinear/time-dependent internal boundary conditions", *J. Sound Vib.*, **330**(22), 5382-5400.
Ghayesh, M.H., Kazemirad, S. and Reid, T. (2012), "Nonlinear vibrations and stability of parametrically exited systems with cubic nonlinearities and internal boundary conditions: A general solution procedure", *Appl. Math. Model.*, **36**(7), 3299-3311.
Hu, Y.J., Yang, J. and Kitipornchai, S. (2010), "Pull-in analysis of electrostatically actuated curved micro-beams with large deformation", *Smart Mater. Struct.*, **19**(6), 065030.
Ibrahimbegović, A. and Al Mikdad, M. (2000), "Quadratically convergent direct calculation of critical points for 3d structures undergoing finite rotations", *Comput. Method. Appl. M.*, **189**(1), 107-120.
Ibrahimbegović, A., Hajdo, E. and Dolarevic, S. (2013), "Linear instability or buckling problems for mechanical and coupled thermomechanical extreme conditions", *Coupled Syst. Mech.*, **2**(4), 349-374
Jia, X.L., Yang, J., Kitipornchai, S. and Lim, C.W. (2012), "Resonance frequency response of geometrically nonlinear micro-switches under electrical actuation", *J. Sound Vib.*, **331**(14), 3397-3411.
Kim, P., Bae, S. and Seok, J. (2012), "Resonant behaviors of a nonlinear cantilever beam with tip mass subject to an axial force and electrostatic excitation", *Int. J. Mech. Sci.*, **64**(1), 232-257.
Ngo, V.M., Ibrahimbegović, A. and Hajdo, E. (2014), "Nonlinear instability problems including localized plastic failure and large deformations for extreme thermo-mechanical loads", *Coupled Syst. Mech.*, **3**(1), 89-110.
Pamidighantam, S., Puers, R., Baert, K. and Tilmans, H.A.C. (2002), "Pull-in voltage analysis of electrostatically actuated beam structures with fixed–fixed and fixed–free end conditions", *J Micromech. Microeng*, **12**(4), 458.
Saif, M.T.A., Alaca, B.E. and Sehitoglu, H. (1999), "Analytical modeling of electrostatic membrane actuator for micro pumps", *J. Microelectromech. Syst.*, **8**(3), 335-345.
Wang, Y.G., Lin, W.H., Feng, Z.J. and Li, X.M. (2012), "Characterization of extensional multi-layer microbeams in pull-in phenomenon and vibrations", *Int. J. Mech. Sci.*, **54**(1), 225-233.
Younis, M.I. (2011), *MEMS Linear and Nonlinear Statics and Dynamics*, Springer
Younis, M.I., Abdel-Rahman, E.M. and Nayfeh, A. (2003), "A reduced-order model for electrically actuated microbeam-based MEMS", *J. Microelectromech. Syst.*, **12**(5), 672-680.
Zengerle, R., Richter, A. and Sandmaier, H. (1992), "A micro membrane pump with electrostatic actuation", *Micro Electro Mechanical Systems, 1992, MEMS '92, Proceedings. An Investigation of Micro Structures, Sensors, Actuators, Machines and Robot. IEEE*, 4-7 Feb 1992.